

Influence of deuterium-induced volume changes on optical transmission in Fe/V (001) and Cr/V (001) superlattices

S. A. Droulias, O. Grånäs, O. Hartmann, K. Komander, B. Hjörvarsson, M. Wolff, and G. K. Pálsson^{*}
*Division of Materials Physics and Materials Theory, Department of Physics and Astronomy, Uppsala University,
 Box 516, SE-75121 Uppsala, Sweden*



(Received 11 January 2022; revised 29 April 2022; accepted 9 May 2022; published 31 May 2022)

The deuterium-induced changes of the optical transmission in Fe/V (001) and Cr/V (001) superlattices are found experimentally to be dominated by the volume changes of the vanadium layers and thus indirectly linked to concentration. The deuterium-induced expansion is 67% larger in Cr/V 2/14 monolayers (ML) as compared to Fe/V 2/14 ML. This large difference can be explained by a difference in the site of deuterium from tetrahedral in Fe/V to octahedral in Cr/V. First-principles calculations based on this assumption give quantitative agreement with both the measured optical transmission and the deuterium-induced expansion coefficient. Placing hydrogen in the middle of the vanadium layers results in total energies at 0 K that favor tetrahedral occupancy at low concentrations, although the energy difference is of the order of the thermal energy available in the experiments. Hence small changes in strain, defect concentration, and/or vibrational spectrum of the superlattices may tip the balance to octahedral occupancy at low concentrations. Given this link to concentration and the linear scaling, optical transmission can, therefore, be used in a straightforward way to obtain pressure-composition isotherms also in thin metal films that do not undergo metal-insulator transitions upon hydrogenation.

DOI: [10.1103/PhysRevB.105.195438](https://doi.org/10.1103/PhysRevB.105.195438)

Knowledge of the pressure-composition isotherms of metal hydrides is crucial when studying, for example, hydrogen storage in metals, hydrogen embrittlement, and thin-film hydrogen-sensing applications [1–3]. Knowledge of the concentration and its distribution in a film can also be used to measure dynamic properties of hydrogen [4,5] and learn how these can change in the presence of finite size [6]. In the case of thin films, optical transmission has been used to measure concentration for about two decades [1,2,4,5,7–10]. The method was originally applied to systems where strong metal-insulator transitions were present, thereby simplifying the interpretation, since the relative volume fraction of the transparent phase is proportional to the concentration [7]. In recent years, optical transmission has also been used for thin metal hydrides that do not undergo metal-insulator transitions [9,10], under the assumption that the scaling of transmission with respect to concentration is known. In this work we revise the fundamental understanding of the underlying mechanism for this technique. Understanding the underlying mechanism for this technique is important since thermodynamic analysis rests on the ability to map the optical transmission to concentration.

To determine the thermodynamic quantities of a thin metal hydride, it is required to determine the concentration as a function of pressure and temperature. The optical transmission is often equated to the concentration via the Lambert-Beer law [9,10]:

$$I(c) = I_0 e^{-\alpha(c,\lambda)d} \rightarrow c = (d\Delta\alpha)^{-1} \ln \frac{I(c)}{I(0)}, \quad (1)$$

where λ is the wavelength of the light, I_0 is the incident intensity, $I(c)$ is the measured transmitted intensity and deuterium concentration c , d is the thickness of the sample, and α is the wavelength and concentration-dependent linear absorption coefficient. The assumptions underlying this law are that the changes in the absorption coefficient are known as a function of concentration and multiple reflections and scattering can be neglected. To find the relationship between optical transmission and concentration the samples need to have high crystal quality, such that effects arising from grain boundaries and other imperfections can be minimized. We also need to separate concentration from the volume expansion that is associated with the uptake of hydrogen. We have chosen vanadium as the material for this study, since it can be grown with high crystal quality as part of a superlattice with either iron or chromium. Vanadium absorbs hydrogen and deuterium readily at room temperature and several phases can be found depending on the concentration and temperature. At low concentration and high temperature, the hydrogen forms a solid solution with vanadium where hydrogen occupies tetrahedral sites, yet retaining the crystal symmetry [11]. At higher concentrations and lower temperature, a hydride phase, the β_1 phase, forms with a change in crystal structure to body-centered tetragonal and octahedral O_2 site occupancy.

^{*}Corresponding author: gunnar.palsson@physics.uu.se

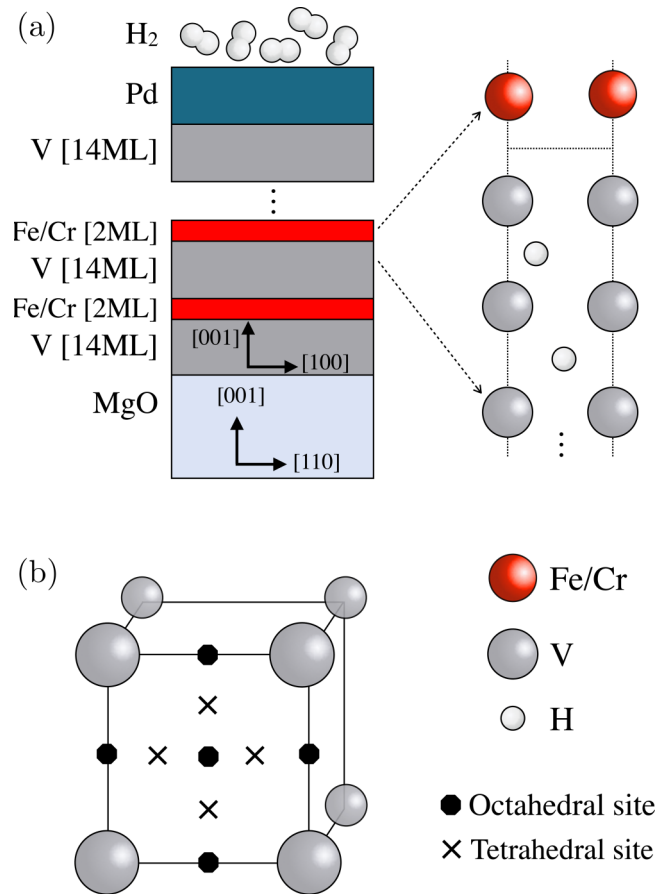


FIG. 1. Panel (a) depicts a schematic of the superlattices including the thickness of the layers and their relative orientation. Panel (b) shows the possible sites for hydrogen and deuterium to occupy inside the two superlattices, tetrahedral or octahedral. ML stands for monolayer.

In this work we work exclusively at high temperatures and are above any phase boundaries, and the volume expansion is thus straightforward to interpret. To achieve the highest possible sample quality, we grow a superlattice stack of alternating vanadium layers and nonabsorbing layers. To test the effect of the nonabsorbing layer on the result, we test both iron and chromium. Due to the large difference in enthalpy, ($\Delta H = +0.3$ eV/atom for Fe, $\Delta H = -0.3$ eV/atom for V), one finds deuterium only in the vanadium layers [12]. In Fig. 1 we show schematically a superlattice composed of a vanadium layer and a nonabsorbing layer, either iron or chromium [13], [Fe/V 2/14] $_{N=25}$ and [Cr/V 2/14] $_{N=30}$ with a specially tuned ratio, which corresponds to optimal crystal quality (the notation i/j refers to the number of atomic layers in each material, and the subscript is the number of repeats of the superlattice). The out-of-plane lattice parameters of the individual layers depend on the elastic constants of the individual materials and we find the strain state of the V layer to be identical in both cases within 2% [14–16]. We determine the concentration and the volume changes from *in situ* neutron reflectivity patterns, and we measure simultaneously the optical transmission.

The neutron measurements were done at the reflectometer SuperADAM (ILL), Grenoble, France [17]. The samples were

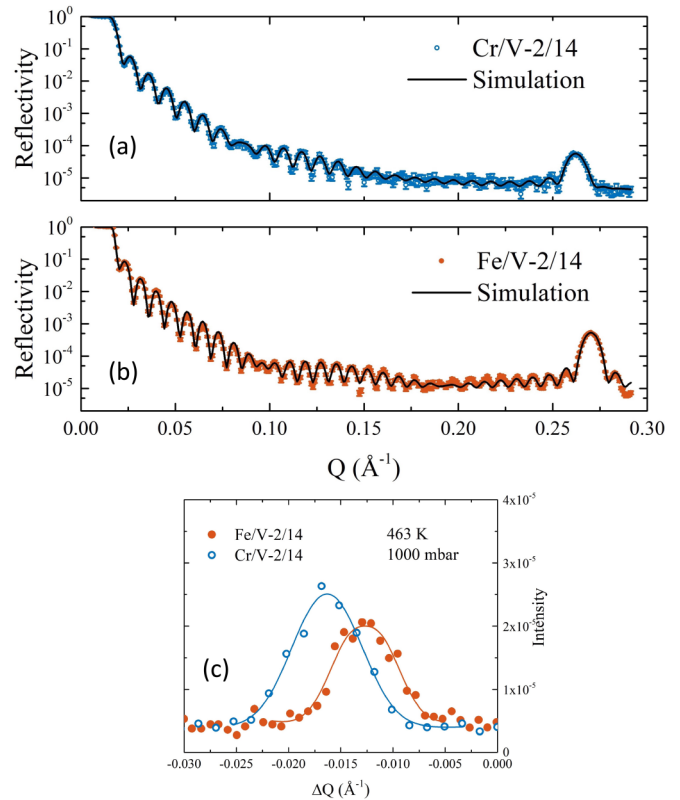


FIG. 2. Neutron reflectivity data from unloaded Cr/V (a) and Fe/V (b) at 463 K and 0 mbar D_2 pressure. Panel (c) shows the difference in position of the first superlattice satellites at 1000 mbar D_2 .

exposed to a deuterium atmosphere of varying pressures, and for each pressure, a reflectivity pattern was measured. Figure 2 shows the neutron reflectivity profiles of the unloaded superlattices [panels (a) and (b)], as well as the change in the position of the first satellite for the two superlattices at 1000 mbar [panel (c)]. As can be seen the peaks have shifted (deuterium-induced expansion) by different amounts and exhibit different intensities, indicating a difference in the deuterium absorption behavior. The intensity of the peak depends primarily on the difference in scattering length density between the layers composing the superlattice. Due to the scattering length density of the deuterated layer changing with deuterium content, the contrast between the layers is also altered. Therefore, the concentration of deuterium in the vanadium layers can be determined by using the intensity of the peak to calculate the scattering length density of the absorbing layer (see Supplemental Material for more information [18]). In this work, the fitting tool GENX [19] was used to fit the whole reflectivity pattern of all pressures. The scattering length density of vanadium is almost zero, which makes it straightforward to find the scattering length density of the iron and chromium layer, which is needed for the calibration. Furthermore, x-ray reflectivity patterns that extend much further in Q were also fitted (not shown) to get an unambiguous structural model for each superlattice [14].

Figure 3 shows the deuterium concentration versus the volume change of the two superlattices. Both superlattices

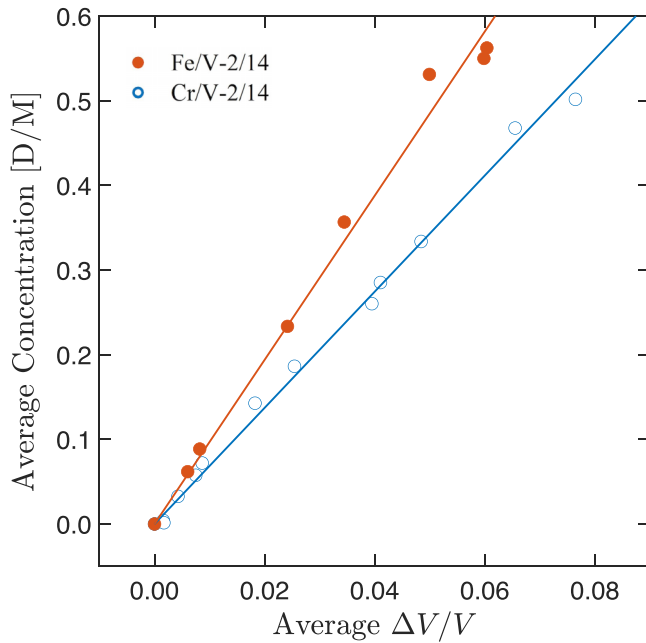


FIG. 3. The figure shows the relationship between the deuterium concentration and the observed volume changes, which is linear for both Fe/V 2/14 and Cr/V 2/14, however, with quite different slopes.

exhibit a linear expansion, as expected when the deuterium is dissolved into the lattice gas phase. Markedly different slopes are seen, which confirms the fact that the two superlattices have different expansion coefficients k . We point out that volume changes and changes in deuterium concentration can be easily distinguished from one another since volume changes mainly shift the reflectivity pattern, and changes of concentration mainly influence intensities. One should note that the deuterium loading of Fe/V and Cr/V superlattices is completely structurally reversible, even after many loading cycles. Cracking, and/or peeling, due to in-plane lattice parameter changes can thus be completely neglected as expected from other findings in the literature of hydrogen in epitaxial films [20,21].

Figure 4 shows the deuterium concentration versus the simultaneously determined optical transmission ($\lambda = 625$ nm) for the two superlattices. As can be seen in the figure, the transmitted intensity is indeed linear for both superlattices. The optical transmission has been scaled by the number of periods in each superlattice to account for a slight change in total thickness. Note that the slope is different between the two superlattices, indicating that the conversion factor between optical transmission and concentration is different.

We see from the data presented in Fig. 4 together with the data presented in Fig. 3 that there is a strong correlation between volume change and the optical transmission, which suggests a common cause. To further understand the influence of volume expansion on optical transmission we have undertaken a first-principle study to calculate the dielectric tensor as a function of the c/a ratio. We calculate the dielectric function for a single unit cell of vanadium for c/a ratios going from 1.0 to 1.1 while keeping the in-plane lattice parameters fixed at the experimentally clamped values. This mimics

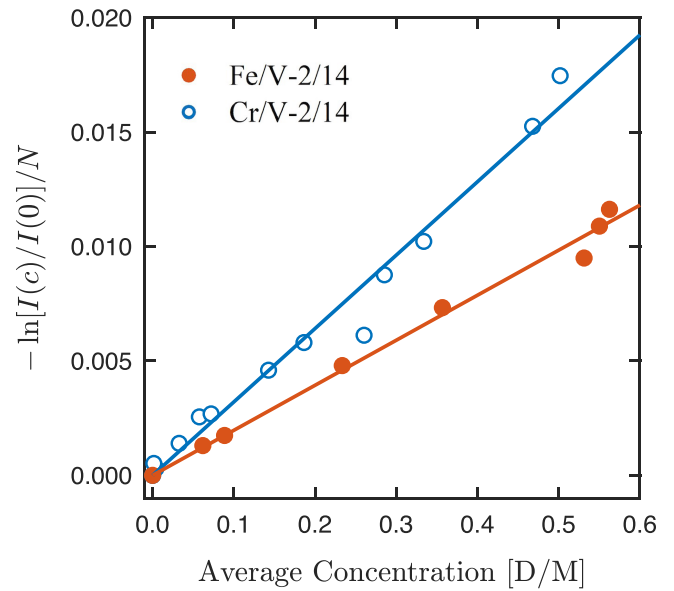


FIG. 4. The figure shows the scaling between the deuterium concentration and the optical transmission. The optical transmission has been scaled by the number of repeats in each superlattice to compensate for a slight difference in thickness.

both the one-dimensional nature of the volume change in the superlattices and the expansion caused by deuterium. In this way we investigate only the volume aspects of the deuterium absorption. The calculated dielectric function is shown in the Supplemental Material together with experimental data and is found to be in good agreement with experiment and previous theory [18,22–25].

Figure 5 shows the relationship between the volume expansion and the optical transmission together with the theoretical results (solid black line). We obtain excellent agreement with the experimental data, which strongly suggests that volume effects drive the observed changes in transmission when deuterium is absorbed, rather than rearrangements of electronic states around the Fermi level. This would imply that, for metals that do not undergo metal-insulator transitions, the linearity between concentration and optical transmission is due to changes in the electron density. This finding is also consistent with the fact that most of the changes to the electronic structure due to deuterium absorption take place around 7 eV below the Fermi level, where the spectral weight owing to s - d hybridization is located [26,27]. Hence, for optical measurements in the visible range, such changes do not contribute to the optical response.

Figure 6 shows the changes in the band structure in selected symmetry directions as the vanadium crystal is stretched, while keeping the in-plane lattice parameter constant, as well as the subsequent changes to the dielectric function. As the volume expands, and the film is strained, the orbital overlap is changed, inducing a change in bandwidth. The trends regarding the nontrivial changes in the optical properties, as produced by first-principles calculations, can be of guidance in determining the most suitable optical frequencies to measure deuterium-induced changes in other materials.

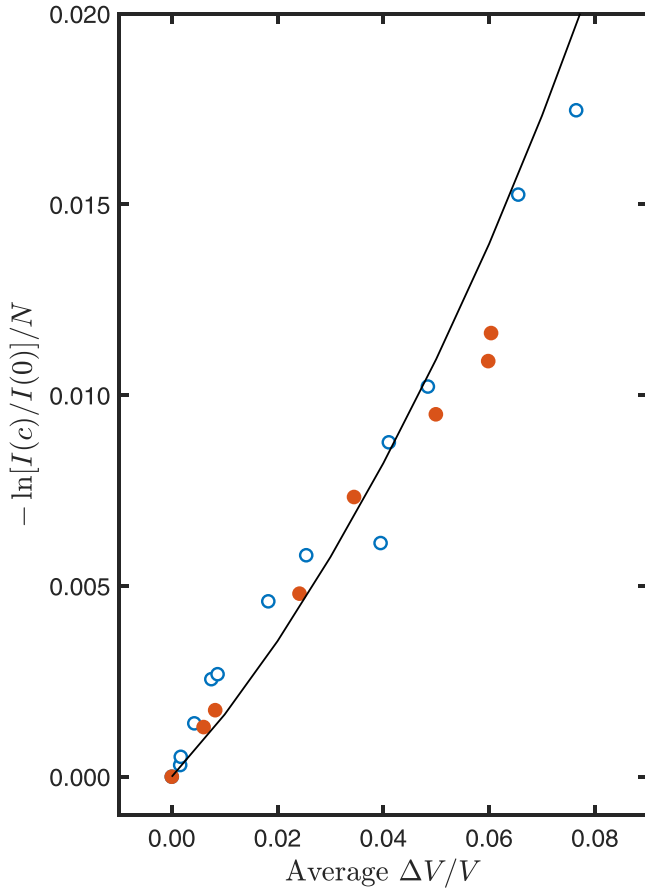


FIG. 5. The figure shows the scaling between the simultaneously measured optical transmission and the one-dimensional volume changes. The solid line in the figure is obtained from a transmission calculation of a 50-nm V film on MgO using the optical constants from the first-principle calculations discussed below. No fitting has been done to adjust the curve to the data.

To obtain a better understanding of the observed expansion coefficient, we have calculated the elastic compliance constants and atomic volumes for both superlattices from first principles. The expansion coefficient in a clamped superlattice is given by (see the Supplemental Material [18,28–30])

$$\frac{\Delta V}{V} \Big|_{\text{clamped}} = kc = \frac{c}{\Omega} \frac{(s_{11}s_{33} + s_{12}s_{33} - 2s_{13}s_{13})}{s_{11} + s_{12}} A, \quad (2)$$

where s_{ij} are the elastic compliance constants of the superlattice in question, c is the deuterium concentration, Ω is the atomic volume of the host, and A is the dipole force component due to deuterium in the z direction. The calculation yielded compliance constants for Fe/V 2/14: $s_{11} = 5.553 \times 10^{-12} \text{ Pa}^{-1}$, $s_{12} = -2.106 \times 10^{-12} \text{ Pa}^{-1}$, $s_{13} = -1.764 \times 10^{-12} \text{ Pa}^{-1}$, and $s_{33} = 5.296 \times 10^{-12} \text{ Pa}^{-1}$. For Cr/V 2/V14, the calculation yields $s_{11} = 4.855 \times 10^{-12} \text{ Pa}^{-1}$, $s_{12} = -1.567 \times 10^{-12} \text{ Pa}^{-1}$, $s_{13} = -1.709 \times 10^{-12} \text{ Pa}^{-1}$, and $s_{33} = 5.170 \times 10^{-12} \text{ Pa}^{-1}$. The shear constants were also calculated but are not needed to calculate expansion. The expansion coefficients can then be calculated using Eq. (2) if the value for the dipole force component A is known. By assuming that deuterium occupies tetrahedral z sites in

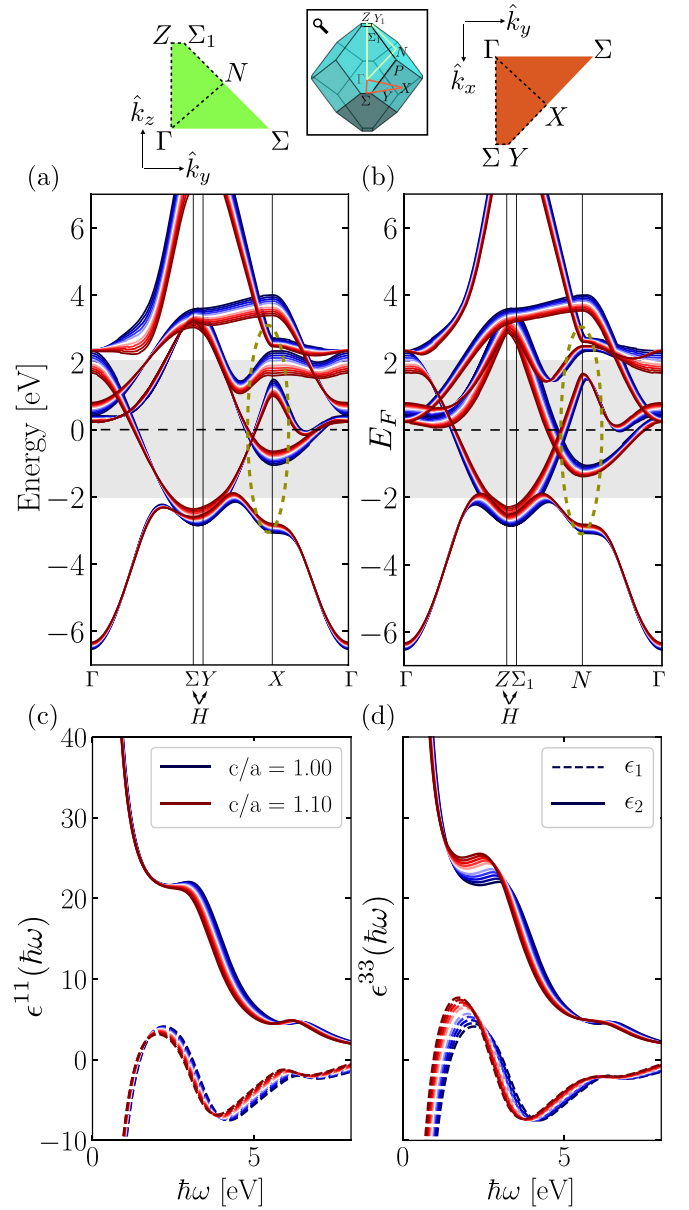


FIG. 6. Panel (a) shows the electronic band-structure in the x - z plane and panel (b) shows a cut in the x - y plane. The respective paths connecting the high symmetry points in the respective plane is schematically illustrated above each panel in green and red, respectively. A three-dimensional representation of the Brillouin zone including both paths is found between the two. The structural distortion leads to a breaking of symmetry indicated by the splitting of the H point in the Brillouin zone path on the horizontal axis. The color coding of the electronic structure indicates the influence of changes in the c/a ratio, where blue corresponds to $c/a = 1.00$ and red refers to $c/a = 1.10$. The gray region indicates the energy range where relevant optical transitions take place. The brown dashed ellipse highlights a region in the Brillouin zone where the structural distortion leads to the observed changes in the dielectric tensor. Panels (c) and (d) show the real and imaginary parts of the dielectric tensor for both in-plane and out-of plane components as a function of the c/a ratio. The color coding of the lines represents the c/a ratio ranging from $c/a = 1.00$ (blue) to $c/a = 1.10$ (red).

TABLE I. Deuterium expansion coefficients of Fe/V and Cr/V superlattices as measured with neutron reflectometry and calculated using first-principles density functional theory, taking into account clamping and symmetry. The middle column refers to the free, three-dimensional volume change. The column on the right refers to a clamped, one-dimensional volume expansion, as found in many thin films.

	$\frac{1}{c} \frac{\Delta V}{V} _{\text{free}}$	$\frac{1}{c} \frac{\Delta V}{V} _{\text{clamped}}$
Experiment Fe/V 2/14		0.103(3)
Experiment Cr/V 2/14		0.168(3)
Calculation	T_z tetrahedral z	
Bulk V	0.194	0.132
Fe/V 2/14	0.157	0.107
Cr/V 2/14	0.150	0.104
	O_z octahedral z	
Bulk V	0.171	0.191
Fe/V 2/14	0.139	0.154
Cr/V 2/14	0.135	0.150

Fe/V and octahedral z sites in Cr/V, and thereby taking the numerical values for the A component (see Supplemental Material [18]), we can calculate corresponding expansion coefficients, which are tabulated in Table I. By taking into account the symmetry of the superlattices, the nonabsorbing layer, and the clamping, we obtain good agreement with the experimental values, only if we assume deuterium occupies tetrahedral z sites in Fe/V and octahedral O_z sites in Cr/V. Further details regarding the elastic constants can be found in the Supplemental Material [18]. To test whether this choice is reasonable, we have compared the total energy from density functional theory calculations at 0 K of one hydrogen atom at a tetrahedral site to a hydrogen atom occupying an octahedral site. The superlattice structure and the strain associated with adhesion to the substrate break the cubic symmetry of the vanadium layer, however, resulting in a large number of unique positions (28), for which total energies and energy barriers have to be calculated. Due to the broken symmetry of superlattice structures, the interstitial sites are, therefore, no longer exactly equivalent. We have calculated the total energy (at 0 K) for hydrogen occupying the central-most sites (see Fig. 2 of the Supplemental Material [18]) and find a 0.2-meV energy difference for Fe/V and a 73-meV energy difference for Cr/V, respectively. In both cases the energy for the tetrahedral occupancy is lower, although the favorability is less so for Fe/V. These energy differences can be compared to the activation energy for the diffusion of hydrogen in bulk vanadium which is 45 meV and the thermal energy available under the experimental conditions, which is 41 meV. As a final point of comparison, the experimental enthalpy of solution was determined from the pressure composition isotherms and was found to be $-0.33(2)$ eV/H atom for both superlattices.

This can be compared to the calculated enthalpies which are -0.285 eV/H atom for Cr/V and -0.281 eV/H atom for Fe/V, both for tetrahedral occupancy. The agreement is good considering the calculations are performed at 0 K and do not include zero-point effects. These results are consistent with a very small energy difference between the two types of sites in both superlattices.

We therefore draw the conclusion that small changes in, for example, strain, zero-point energies, and/or the phonon spectrum can easily tip the balance from tetrahedral to octahedral occupancy at low concentrations. Hence, it is not at all surprising to see different occupancies in seemingly similar materials at low concentrations. To calculate the full energy spectrum of all the different types of sites, including zero-point energies, phonon dispersion, and deuterium-deuterium interaction, will be left to future work. The ultimate reason for deuterium occupying different sites in the seemingly similar lattices highlights the effect proximity can have on materials' properties. In the present case we suggest that subtle differences in the elastic response of the lattice may tip the energy balance between which site is preferred. This difference is reinforced by the one-dimensional character of the expansion.

We find from simultaneous neutron reflectometry and optical transmission experiments that the optical transmission scales linearly with deuterium concentration at $\lambda = 625$ nm for both superlattices but with different slopes. The origin of this linearity is traced to the changes in volume that cause changes in the electron density, which are confirmed by first-principle calculations. We can understand why the volume expansion is so different in the two superlattices by assuming that deuterium occupies tetrahedral z sites in Fe/V and octahedral z sites in Cr/V. A full understanding of the influence of deuterium-deuterium interaction on site occupancy is, however, needed to obtain a complete picture in these structures.

These findings imply that metal hydride films, even without exhibiting metal-insulator transitions during hydrogenation, can be measured using optical transmission as long the volume expansion of the hydride is taken into account. For example, in a material that undergoes a change from tetrahedral to octahedral occupancy, like the transition from the α - β_1 phase in vanadium, the scaling factors for the optical transmission to concentration will be different on either side of the phase boundary.

The work of O.G. was supported by the Swedish Foundation for Strategic Research (SSF) under Grant No. ICA16-0037. The computations were enabled by resources provided by the Swedish National Infrastructure for Computing (SNIC), partially funded by the Swedish Research Council through Grant Agreement No. 2018-05973. The SuperADAM project acknowledges the Swedish research council for support.

- [1] J. N. Huiberts, R. Griessen, J. H. Rector, R. J. Wijngaarden, J. P. Dekker, D. G. de Groot, and N. J. Koeman, *Nature (London)* **380**, 231 (1996).
 [2] X. Xin, G. K. Pálsson, M. Wolff, and B. Hjörvarsson, *Phys. Rev. Lett.* **113**, 046103 (2014).

- [3] C. Boelsma, L. J. Bannenberg, M. J. Van Setten, N. J. Steinke, A. A. van Well, and B. Dam, *Nat. Commun.* **8**, 15718 (2017).
 [4] F. J. A. den Broeder, S. J. van der Molen, M. Kremers, J. N. Huiberts, D. G. Nagengast, A. T. M. van Gogh, W. H. Huisman, N. J. Koeman, B. Dam, J. H. Rector, S. Plota, M. Haaksma,

- R. M. N. Hazen, R. M. Jungblut, P. A. Duine, and R. Griessen, *Nature (London)* **394**, 656 (1998).
- [5] G. K. Pálsson, A. Bliersbach, M. Wolff, A. Zamani, and B. Hjörvarsson, *Nat. Commun.* **3**, 892 (2012).
- [6] W. Huang, G. K. Pálsson, M. Brischetto, H. Palonen, S. A. Droulias, O. Hartmann, M. Wolff, and B. Hjörvarsson, *New J. Phys.* **19**, 123004 (2017).
- [7] A. Borgschulte, W. Lohstroh, R. Westerwaal, H. Schreuders, J. Rector, B. Dam, and R. Griessen, *J. Alloys Compd.* **404**, 699 (2005).
- [8] B. Dam, R. Gremaud, C. Broedersz, and R. G. Materialia, *Scr. Mater.* **56**, 853 (2007).
- [9] R. Gremaud, M. Slaman, H. Schreuders, B. Dam, and R. Griessen, *Appl. Phys. Lett.* **91**, 231916 (2007).
- [10] J. Prinz, G. K. Pálsson, P. T. Korelis, and B. Hjörvarsson, *Appl. Phys. Lett.* **97**, 251910 (2010).
- [11] J. Bloch, B. Pejova, J. Jacob, and B. Hjörvarsson, *Phys. Rev. B* **82**, 245428 (2010).
- [12] G. Alefeld and J. Vökl, *Hydrogen in Metals I* (Springer-Verlag, Berlin, 1978).
- [13] A. Liebig, G. Andersson, J. Birch, and B. Hjörvarsson, *Thin Solid Films* **516**, 8468 (2008).
- [14] S. A. Droulias, G. K. Pálsson, H. Palonen, A. Hasan, K. Leifer, V. Kapaklis, B. Hjörvarsson, and M. Wolff, *Thin Solid Films* **636**, 608 (2017).
- [15] J. Birch, J.-E. Sundgren, and P. Fewster, *J. Appl. Phys.* **78**, 6562 (1995).
- [16] S. Olsson and B. Hjörvarsson, *Phys. Rev. B* **71**, 035414 (2005).
- [17] A. Vorobiev, A. Devishvilli, G. Pálsson, H. Rundlof, N. Johansson, A. Olsson, A. Dennison, M. Wolff, B. Giroud, O. Aguetaz, and B. Hjörvarsson, *Neutron News* **26**, 25 (2015).
- [18] See Supplemental Material at <http://link.aps.org/supplemental/10.1103/PhysRevB.105.195438> for a description of the sample, the neutron instrument, theoretical details, and effects of clamping on volume change.
- [19] M. Björck and G. Andersson, *J. Appl. Crystallogr.* **40**, 1174 (2007).
- [20] G. Song, A. Remhof, K. Theis-Bröhl, and H. Zabel, *Phys. Rev. Lett.* **79**, 5062 (1997).
- [21] G. K. Pálsson, A. R. Rennie, and B. Hjörvarsson, *Phys. Rev. B* **78**, 104118 (2008).
- [22] F. Sacchetti, *J. Phys. F* **13**, 1801 (1983).
- [23] J. Weaver, D. Lynch, and C. Olson, *Phys. Rev. B* **10**, 501 (1974).
- [24] D. G. Laurent, C. S. Wang, and J. Callaway, *Phys. Rev. B* **17**, 455 (1978).
- [25] P. Romaniello, P. L. de Boeij, F. Carbone, and D. van der Marel, *Phys. Rev. B* **73**, 075115 (2006).
- [26] H. Smithson, C. A. Marianetti, D. Morgan, A. Van der Ven, A. Predith, and G. Ceder, *Phys. Rev. B* **66**, 144107 (2002).
- [27] G. K. Pálsson, A. K. Eriksson, M. Amft, X. Xin, A. Liebig, S. Ólafsson, and B. Hjörvarsson, *Phys. Rev. B* **90**, 045420 (2014).
- [28] G. K. Pálsson, M. Wälde, M. Amft, Y. Wu, M. Ahlberg, M. Wolff, A. Pundt, and B. Hjörvarsson, *Phys. Rev. B* **85**, 195407 (2012).
- [29] G. Kresse and J. Furthmüller, *Phys. Rev. B* **54**, 11169 (1996).
- [30] G. Kresse and D. Joubert, *Phys. Rev. B* **59**, 1758 (1999).